

Actin and Myosin Function in Directed Vacuole Movement during Cell Division in *Saccharomyces cerevisiae*

Kent L. Hill, Natalie L. Catlett, and Lois S. Weisman

Department of Biochemistry, University of Iowa, Iowa City, Iowa 52242

Abstract. During cell division, cytoplasmic organelles are not synthesized de novo, rather they are replicated and partitioned between daughter cells. Partitioning of the vacuole in the budding yeast *Saccharomyces cerevisiae* is coordinated with the cell cycle and involves a dramatic translocation of a portion of the parental organelle from the mother cell into the bud. While the molecular mechanisms that mediate this event are unknown, the vacuole's rapid and directed movements suggest cytoskeleton involvement. To identify cytoskeletal components that function in this process, vacuole inheritance was examined in a collection of actin mutants. Six strains were identified as being defective in vacuole inheritance. Tetrad analysis verified that the defect cosegregates with the mutant actin gene. One strain with a deletion in a myosin-binding region was

analyzed further. The vacuole inheritance defect in this strain appears to result from the loss of a specific actin function; the actin cytoskeleton is intact and protein targeting to the vacuole is normal. Consistent with these findings, a mutation in the actin-binding domain of Myo2p, a class V unconventional myosin, abolishes vacuole inheritance. This suggests that Myo2p serves as a molecular motor for vacuole transport along actin filaments. The location of actin and Myo2p relative to the vacuole membrane is consistent with this model. Additional studies suggest that the actin filaments used for vacuole transport are dynamic, and that profilin plays a critical role in regulating their assembly. These results present the first demonstration that specific cytoskeletal proteins function in vacuole inheritance.

THE cytoplasm of eukaryotic cells is distinguished by the presence of numerous membrane-bound organelles that carry out specific and essential cellular functions. These organelles are complex structures that are not readily synthesized de novo. Hence, during cell division each new cell does not synthesize its own set of organelles, rather the organelles present in the parental cell are replicated and then partitioned between daughter cells before cytokinesis (54). The coordination of organelle partitioning with the cell cycle, together with the accuracy and efficiency of this process, strongly suggests the involvement of active partitioning mechanisms. A few proteins have recently been implicated in organelle inheritance through biochemical (19, 20, 60) and genetic approaches (34, 44, 53, 58, 61). However, the underlying molecular mechanisms remain to be established.

Organelle inheritance has been studied in a variety of systems and it appears that the mechanisms involved vary among different organisms, as well as for different organelles within the same cell. During mitosis in mammalian cells, the ER and Golgi apparatus become fragmented, forming many small vesicles that are specifically

divided between daughter cells and then reassembled, leaving each new cell with its own complete set (54). Fragmentation is thought to aid in the equal partitioning of these organelles, although it is not clear whether this partitioning is stochastic or whether it requires the function of specific proteins. In the budding yeast *Saccharomyces cerevisiae*, organelles such as the nucleus, vacuole, and mitochondria do not undergo fragmentation. Therefore, the faithful inheritance of these low copy structures absolutely requires that they be actively partitioned between the mother and daughter cell before cytokinesis (54). Interestingly, although partitioning of these organelles might be expected to use common components, many of the proteins involved appear to be unique, since mutants that are defective in the inheritance of one organelle often show normal partitioning of others (34, 44, 53, 56, 58).

Inheritance of the vacuole in *S. cerevisiae* serves as an excellent model for studying organelle inheritance. This event begins early in the cell cycle and is marked by the formation of a tubular-vesicular "segregation structure" that extends from the parental organelle into the bud (55, 57). Translocation of the segregation structure from the mother cell into the bud proceeds along a specific path at a rate of 0.1–0.2 $\mu\text{m/s}$ (Weisman, L.S., unpublished). Once established, the segregation structure allows for the transfer of vacuolar material between mother and daughter

Please address all correspondence to L.S. Weisman, Department of Biochemistry, University of Iowa, Iowa City, IA 52242. Tel.: (319) 335-8581. Fax: (319) 335-9570. E-Mail: lois-weisman@uiowa.edu

cells. Eventually, this structure disappears as the nucleus migrates into the neck region between the mother cell and the bud (24).

One feature of vacuole inheritance that distinguishes it from other membrane trafficking pathways, such as secretion and endocytosis, is that it requires the delivery of a membrane-enclosed structure to a subcellular location that does not contain a pre-existing acceptor membrane. Therefore, not only must this event be precisely coordinated with the cell cycle, but it must also be spatially constrained so as to provide for targeting of the inherited organelle to the correct subcellular location. This targeting might be achieved via directed transfer of the organelle (or heritable unit) along a specific, predefined path, and/or by marking the ultimate destination such that the organelle is specifically retained once it arrives. Directed movements of eukaryotic organelles are generally mediated by cytoskeletal proteins. Examples include the transport of cytoplasmic vesicles in neurons (3) and the segregation of centrosomes during mitosis (5), both of which are microtubule-mediated events. Partitioning of the vacuole in *S. cerevisiae*, however, is probably not dependent on microtubules, since treatment with nocodazole does not block vacuole inheritance (14, 16). Actin microfilaments have also been demonstrated to function in intracellular organelle movements (6, 30, 45). To determine whether actin might be involved in vacuole partitioning, we examined several yeast strains carrying mutations in the actin structural gene, or in genes encoding known actin-binding proteins. Our results present the first identification of specific cytoskeletal components involved in vacuole inheritance.

Materials and Methods

Strains, Growth Conditions, and Genetic Manipulations

Yeast strains used in this study are listed in Table I. Unless otherwise indicated cultures were grown at 24°C in YEPD¹ medium (25). Where indicated cells were grown in synthetic complete (SC) medium (25) lacking the appropriate amino acids. Standard yeast genetic techniques were performed as described (25). Yeast transformations were done according to the procedure of Gietz et al. (13).

In Vivo Labeling of Vacuoles

For measuring vacuole inheritance, vacuoles were labeled in vivo with *N*-(3-triethylammoniumpropyl)-4-(*p*-diethylaminophenyl)hexatrienyl (FM4-64) (Molecular Probes, Eugene, OR) according to the method of Vida et al. (50). Briefly 0.1–0.2 OD₆₀₀ U of cells were harvested from log phase cultures, resuspended in 0.25 ml of YEPD medium containing 80 μM FM4-64, and incubated for 1 h at 24°C with shaking. After labeling, cells were washed twice, resuspended in 5 ml of fresh medium, and incubated for an additional 2.5–4 h. This chase period was sufficient to allow for at least one cell doubling as verified by OD₆₀₀ measurements. After the chase period cells were collected by low speed (800 g) centrifugation and examined by fluorescence microscopy using a Zeiss Axioskop fluorescence microscope, equipped with an MC 100 35-mm camera.

For zygote experiments, 2 OD₆₀₀ U of the indicated parental strains were labeled as described above, and then washed and incubated in fresh medium for 1 h at 24°C with shaking. After 1 h, labeled cells (~1 OD₆₀₀ U) were mixed with an equal number of unlabeled cells of the opposite mating type, incubated with shaking at 24°C for 1 h, and then plated onto

YEPD plates and placed in the dark. After 2.5–3.5 h in the dark, zygotes were scraped from the plate, resuspended in 4 μl of YEPD medium on a glass slide and examined by fluorescence microscopy as above.

For the cell sorting experiment shown in Fig. 2, 1-ml samples were removed at the indicated time points during the chase and analyzed using an EPICS 753 Fluorescence-Activated Cell Sorter (Coulter Electronics, Inc., Hialeah, FL). Cells were excited at 488 nm and emitted light was detected with a 670/14 band pass filter. For each sample 10⁴ cells were analyzed.

Phalloidin Staining of F-actin

Phalloidin labeling of F-actin in fixed cells was done according to the method of Adams and Pringle (2). Briefly, log phase cells were fixed with 3.7% formaldehyde in growth medium for 60 min at room temperature, then washed three times with PBS (2) and resuspended in 0.1 ml of PBS. FITC-phalloidin (Molecular Probes) was added from a methanolic stock solution to a final concentration of 1.1 μM and cells were incubated in the dark at room temperature for 2–2.5 h. Labeled cells were washed five times with PBS before examination by fluorescence microscopy.

Indirect Immunofluorescence Localization

For all experiments, cells were fixed by the addition of 37% formaldehyde directly to the growth medium to a final concentration of 3.7%. Fixation was carried out with minimal shaking for 3 h. Spheroplasts were made by incubating fixed cells in 1.2 M sorbitol, 0.1 M potassium phosphate, pH 6.5, 1% β-mercaptoethanol with 10 μg/ml oxalyticase (Enzogenetics, Eugene, OR) for 10–15 min (80–90% of cells formed spheroplasts as assessed by phase contrast microscopy). Washed spheroplasts were attached to 1% polyethylenimine-coated multiwell slides (ICN Biomedicals, Aurora, OH). Standard blocking buffer and wash conditions were used (25). In all cases, localization of the vacuole membrane was achieved using an anti-60-kD ATPase mouse monoclonal antibody (Molecular Probes) at a dilution of 1:50 followed by Lissamine rhodamine-conjugated donkey anti-mouse IgG (Jackson ImmunoResearch Labs, Inc., West Grove, PA) at a dilution of 1:200.

We found that the actin cables could not be adequately detected with fluorescent phalloidin conjugates in cells which had been fixed and spheroplasted. Consequently, we tested the use of rabbit anti-yeast actin antibody for simultaneous localization of actin and the vacuole membrane. Clear visualization of actin cables by immunofluorescence requires that the cells be pretreated with cold (–20°C) methanol for 6 min, followed by –20°C acetone for 30 s (10). Although the methanol/acetone treatment is not compatible with the immunofluorescence localization of several antigens, the ATPase staining was not affected by this treatment. Actin was visualized by a 2-h incubation with rabbit anti-yeast actin antibody (32) (1:10 dilution) followed by a 1-h incubation with Oregon Green 488 conjugated goat anti-rabbit IgG (Molecular Probes) (1:200 dilution). Affinity purification of anti-actin antibody was performed with nitrocellulose blots as described (39).

Simultaneous visualization of Myo2p and the vacuole membrane was performed in yeast zygotes. 2.5 OD₆₀₀ U each of mid-log phase *MATa* and *MATα* strains were mixed together in YEPD medium and shaken at 24°C for 1 h. The cells were then harvested, plated onto YEPD plates, and allowed to incubate at 24°C for an additional 3–4 h. Cells were gently washed from the plate with YEPD and fixed as described above. Myo2p was visualized with affinity-purified rabbit anti-Myo2p antibody followed by antibody amplification as described (32) except that Oregon Green 488 conjugated goat anti-rabbit IgG was used as the final antibody. Affinity-purified anti-Myo2p antibody was generously provided by Drs. S. Lillie and S. Brown (University of Michigan, Ann Arbor, MI). The amplification antibodies were preadsorbed two times to fixed yeast cells and were used at a final dilution of 1:250. In all experiments, omission of the primary antibody resulted in no detectable fluorescence. No cross-reactivity was observed between the anti-mouse and anti-rabbit antibodies.

Stained cells were visualized using an MRC 1024 Scanning Confocal head mounted on a Nikon Optiphot equipped with either a 60× or 100× oil immersion objective, 1.4/NA BioRad Labs (Hercules, CA). The excitation light source used was a mixed gas krypton/argon laser, passed through a dual dichroic filter, allowing excitation at both 488 nm and 568 nm. Dual detection was performed with separate photomultiplier tubes and the resultant images merged using Laser Sharp software. For each field, a z-series of 3–7 1-μm steps was scanned, and projected to a single view. Single steps were also analyzed.

1. Abbreviations used in this paper: SC, synthetic complete medium; vac, vacuole inheritance mutant; YEPD, yeast extract peptone, dextrose medium.

Table 1. Yeast Strains Used

Strain	Genotype	Reference
TDyDD	<i>MATα/MATα, leu2-3, 112//leu2-3, 112, ura3-52/ura3-52, lys2+, ade2+, act1Δ::LEU2+</i>	(8)
LWY1412*	<i>MATα, leu2-3, 112, ura3-52, ACT1</i>	This study
LWY1425*	<i>MATα, leu2-3, 112, ura3-52, ACT1</i>	This study
LWY1408*	<i>MATα, leu2-3, 112, ura3-52, lys2, act1Δ::LEU2, pΔDSE(URA3)</i>	This study
LWY1419*	<i>MATα, leu2-3, 112, ura3-52, act1Δ::LEU2, pΔDSE(URA3)</i>	This study
DDY 338	<i>MATα, ura3-52, leu2-3, 112, his3Δ200, can1-1, tub2-201, cry1, act1-101::HIS3</i>	(59)
DDY339	<i>MATα, ura3-52, leu2-3, 112, his3Δ200, can1-1, tub2-201, act1-102::HIS3</i>	(59)
DDY356	<i>MATα, ura3-52, leu2-3, 112, his3Δ200, can1-1, tub2-201, act1-105::HIS3</i>	(59)
DDY341	<i>MATα, ura3-52, leu2-3, 112, his3Δ200, can1-1, tub2-201, ade2-101, cry1, act1-11::HIS3</i>	(59)
DDY654	<i>MATα, ura3-52, leu2-3, 112, his3Δ200, tub2-201, can1-1, ade4, act1-121::HIS3</i>	(59)
DDY655	<i>MATα, ura3-52, leu2-3, 112, his3Δ200, tub2-201, can1-1, ade4, act1-122::HIS3</i>	(59)
DDY336	<i>MATα, ura3-52, leu2-3, 112, his3Δ200, can1-1, tub2-201, cry1, act1-133::HIS3</i>	(59)
DDY353	<i>MATα, ura3-52, leu2-3, 112, his3Δ200, tub2-201, ade2-101, act1-135::HIS3</i>	(59)
RH2069	<i>MATα, his4, leu2-3, 112, ura3-52, bar1, end7-1</i>	(36)
JP7A	<i>MATα, ura3-51, met6, ade1, his6, leu2-3, 112, myo2-66</i>	(23)
21R	<i>MATα, ura3-52, leu2-3, 112, ade1, MYO2</i>	(23)
myo4ΔU5-2A	<i>MATα, ura3-52, his3, leu2, lys2, trp1, myo4Δ::URA3</i>	(17)
DC5	<i>MATα, ura3-52, lys2, his3, leu2, ade2-201, ade3, PFY1</i>	(18)
BHY31	<i>MATα, ura3-52, lys2, his3, leu2, ade2-201, ade3, pfy1-112::LEU2</i>	(18)

*These strains were generated by sporulation of TDyDD after transformation with plasmid pΔDSE as described by Cook et al. (8).

³⁵S-Labeling and Immunoprecipitation

³⁵S in vivo labeling and immunoprecipitation of carboxypeptidase Y and proteinase A were performed using a modification of the procedure described by Horazdovsky and Emr (21). Cultures were grown to log phase in synthetic complete (SC) medium supplemented with 0.2% yeast extract. Spheroplasts were prepared from 20 OD₆₀₀ U of cells as described by Vida et al. (51), except that SC medium was used instead of WIMPYE, and zymolyase (10 mg/ml) (ICN Pharmaceuticals, Costa Mesa, CA) was used instead of oxalyticase. Spheroplasts were harvested (3,000 g, 3 min), resuspended at 10 OD₆₀₀ U in SC-methionine, -cysteine medium containing 1 M sorbitol, 1 mg/ml BSA, and 0.1 mg/ml α2-macroglobulin (21). Labeling with 150 μCi/ml Tran³⁵S-label (ICN Pharmaceuticals) was carried out for 10 min at 24°C with gentle shaking. The chase was initiated by adding unlabeled methionine (5 mM), cysteine (1 mM) and yeast extract (0.2%); and then incubated for an additional 30 min at 24°C. Aliquots taken before and after the chase period were separated into intracellular and extracellular fractions by centrifugation (15,000 g, 30 s), and then TCA was added to a final concentration of 10%. Dried TCA pellets were resuspended by sonication in resuspension buffer (28). CPY and PrA immunoprecipitations were carried out as described (28), using one wash each with “urea buffer” (100 mM Tris [pH 7.5], 200 mM NaCl, 2 M urea, 0.5% Tween-20) and 0.1% SDS instead of the 1% β-mercaptoethanol wash. Samples were analyzed by SDS 11% polyacrylamide gel electrophoresis and fluorography.

Results

Actin Is Involved in Vacuole Inheritance

Vacuole inheritance was examined by labeling cells with the styryl dye FM4-64. This vital fluorophore specifically stains the vacuolar membrane, and is stable for several generations (50). Labeled cells were viewed by fluorescence microscopy after incubation for a minimum of one cell doubling time in fresh medium without the fluorophore. In this type of “pulse-chase” experiment, buds that form during the chase period will only be labeled if they have inherited a fluorescent vacuole from the labeled parent. In wild-type cells virtually every bud inherits a vacuole and in many cases a pronounced segregation structure can be seen (arrowhead in Fig. 1 a). In an actin mutant (*act1-ΔDSE*; 8), the labeled parental vacuole is not inher-

ited by the daughter cell and segregation structures are not observed (Fig. 1 b). The actin gene in this mutant encodes a truncated actin molecule that lacks the three NH₂-terminal amino acids, and, aside from a slightly decreased ability to support invertase secretion, no phenotype had previously been associated with the *act1-ΔDSE* mutation (8). Note that after the initial portion of the chase period, buds receive the fluorophore exclusively through inheritance. Previous studies have shown that daughter cells that do not inherit a vacuole are nonetheless able to generate a normal vacuole (53, 58), perhaps through Golgi to vacuole vesicle traffic and/or endocytosis. This ability to generate a normal-sized vacuole may account for the virtually wild-type growth rate of *act1-ΔDSE*.

Actin filaments in *S. cerevisiae* cells are found in two characteristic forms, cortical patches at the cell surface and cytoplasmic cables that extend between the mother cell and the bud (1, 27). The cortical patches are most often found in areas experiencing active growth and are thought to function in endocytosis and secretion (35). The function of the cables is unknown. The distribution of filamentous actin in *act1-ΔDSE* cells is similar to wild-type (Fig. 1, c and d). Therefore, the *act1-ΔDSE* mutation does not block vacuole transport by simply disrupting the yeast cytoskeleton. Rather, the inheritance defect in this mutant is probably a direct consequence of impaired actin function.

To probe the extent of the vacuole inheritance defect in *act1-ΔDSE*, we sought to analyze a large population of cells. Logarithmically growing cultures were labeled with FM4-64, and then washed and chased in fresh medium. Samples taken during the chase period were analyzed by Fluorescence Activated Cell Sorting (Fig. 2). As expected, wild-type cells behave primarily as a homogeneous population in which the average fluorescence per cell gradually decreases (53). Vacuole inheritance mutants (*vac*) examined by this method exhibit a characteristic bimodal fluorescence distribution, in which two peaks are observed that correspond to a population of weakly fluorescent

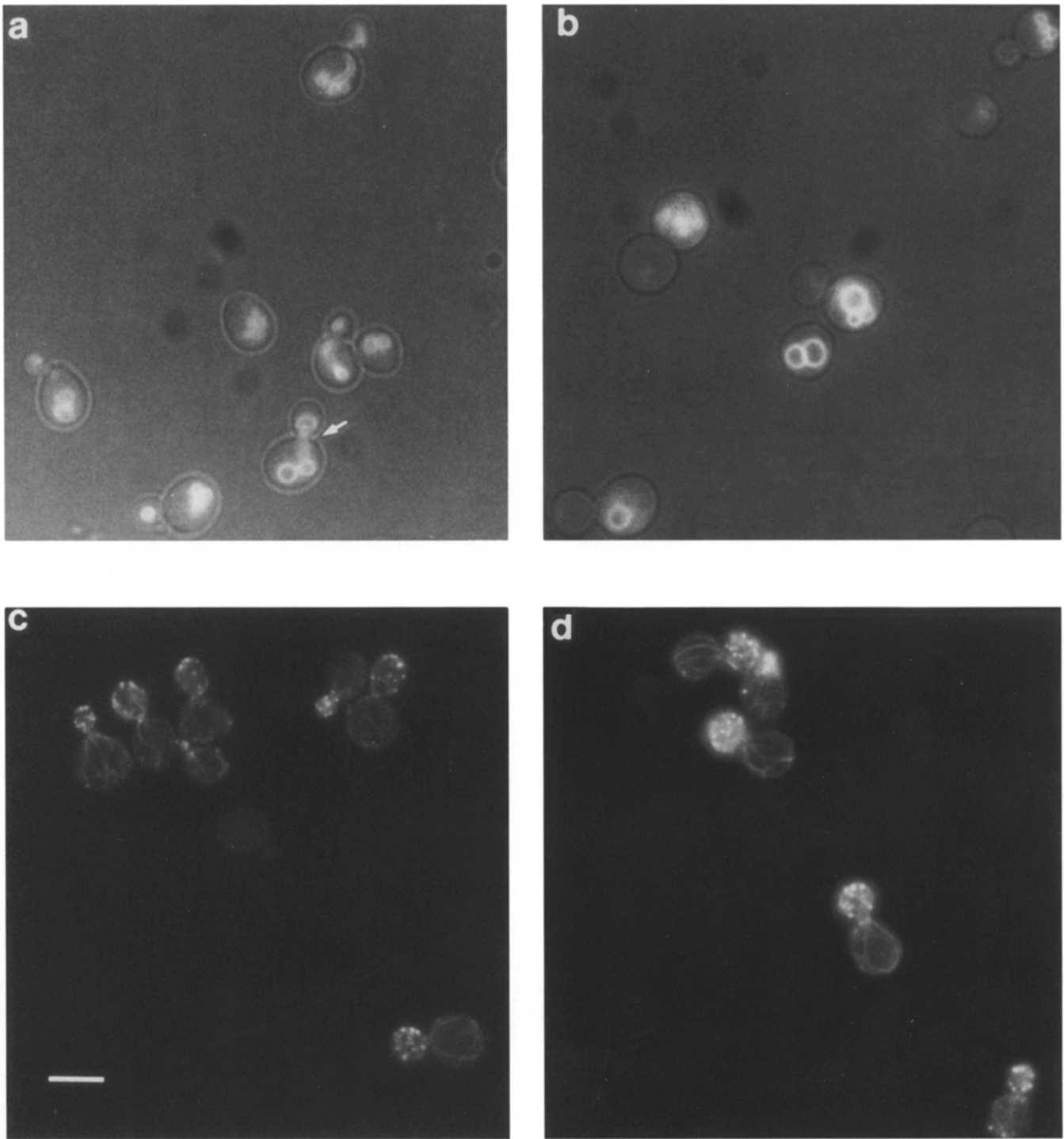


Figure 1. Deletion of the three NH₂-terminal amino acids of actin blocks vacuole inheritance but does not disrupt the overall organization of the actin cytoskeleton. (*a* and *b*) Wild-type (*a*) and *act1-ΔDSE* (*b*) cells were labeled with a vacuole-specific fluorophore as described in Materials and Methods. After labeling, cells were washed two times with fresh medium, resuspended in 5 ml of medium without the fluorophore, incubated for an additional 3 h, and then visualized by fluorescence microscopy. Wild-type buds inherit a labeled vacuole from the parental cell, but buds in the actin mutant do not. Arrowheads mark cells with a segregation structure. (*c* and *d*) To visualize filamentous actin, wild-type (*c*) and *act1-ΔDSE* (*d*) cells were fixed and stained with FITC-phalloidin according to the protocol of Adams and Pringle (1991). The pattern of F-actin staining is similar in wild-type cells and the actin mutant. Bar, 5 μm.

daughter cells that have not inherited a fluorescent vacuole, and a population of highly fluorescent mother cells that have retained their fluorescent vacuoles (53). As seen in Fig. 2, *act1-ΔDSE* cells display a fluorescence profile

that is characteristic of *vac* mutants. Furthermore, the fluorescence intensity of the mother cells in this mutant remains almost unchanged over the course of the experiment (approximately two doubling times), indicating that

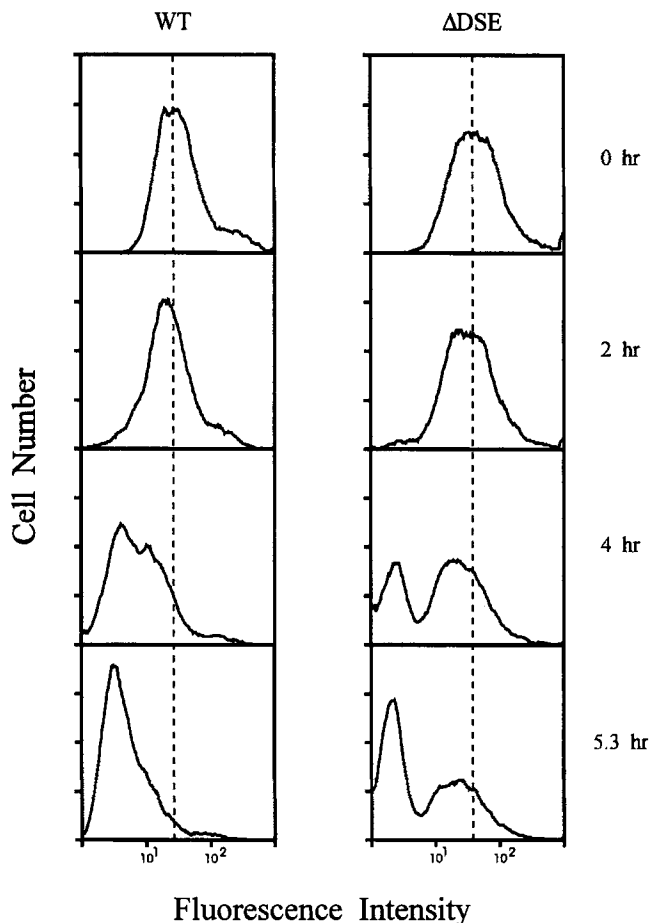


Figure 2. Fluorescence-activated cell sorting profiles of wild-type (WT) and *act1-ΔDSE* (Δ DSE) cells. Cells were labeled with a vacuole-specific fluorophore and chased in fresh medium as described in the legend to Fig. 1. At the indicated time points 1-ml samples were removed and analyzed by fluorescence-activated cell sorting. 10^4 cells were counted for each sample. These results are representative of two independent experiments.

the mother cells retain almost all of their original vacuolar material.

To verify that the *vac* phenotype of *act1-ΔDSE* is due to the mutant actin gene, a hemizygous (*act1Δ::LEU2/ACT1*) diploid, carrying the *act1-ΔDSE* actin gene on a *URA3*-containing plasmid, was sporulated and vacuole inheritance was quantitated in the meiotic progeny (Fig. 3 a). The results demonstrate that the inheritance defect cosegregates with the *act1-ΔDSE* gene. Furthermore this phenotype is recessive, since cells carrying both a mutant and a wild-type actin gene exhibit normal inheritance (see for example, tetrads 2C and 2D in Fig. 3 a). The fact that the *vac* phenotype is recessive is consistent with in vitro studies which demonstrated that wild-type actin can attenuate defects associated with Δ DSE actin when assembled as a copolymer (8).

Vacuole Inheritance Defects in Additional *act1* Alleles

We examined vacuole inheritance in several additional actin mutants. Table II shows the results of this analysis and summarizes other phenotypes that have been reported for

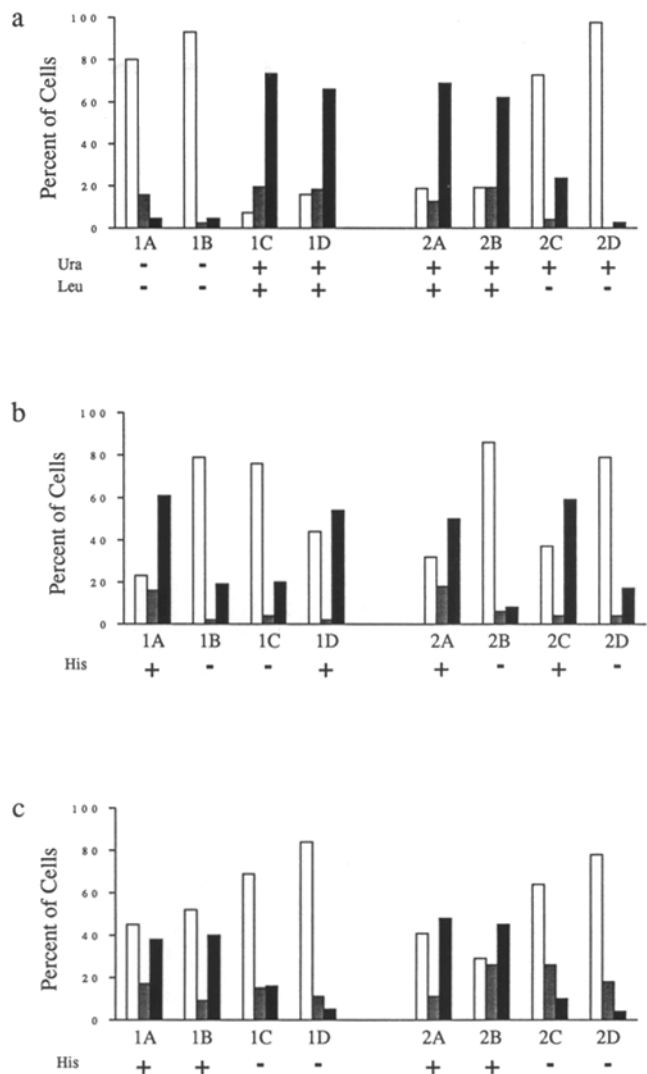


Figure 3. Tetrad analysis demonstrates that a vacuole inheritance defect cosegregates with mutant actin alleles *act1-ΔDSE*, *act1-101*, and *act1-105*. (a) A diploid strain (TDyDD) in which one chromosomal copy of the *ACT1* gene has been replaced with the *LEU2* gene, was transformed with a *URA3*-containing centromeric plasmid (pΔDSE) carrying the *act1-ΔDSE* actin gene (8). A *Ura*⁺ transformant was selected and sporulated. The meiotic progeny were scored for vacuole inheritance as well as for the presence of the pΔDSE plasmid (*Ura*⁺) and the disrupted (*act1::LEU2*) chromosomal actin gene (*Leu*⁺). (b and c) Mutant strains carrying the *act1-101* (b) or *act1-105* (c) alleles were back-crossed to congenic wild-type strains. The resulting diploid strains were sporulated and scored for vacuole inheritance as above. The presence of the mutant (*His*⁺) or wild type (*His*⁻) actin allele was also determined. To quantitate vacuole inheritance, random fields of cells with a labeled vacuole in the mother cell were analyzed. A minimum of 50 cells were scored for each strain. (Open bars) Buds that inherited normal amounts of the parental vacuole. (Stippled bars) Buds that inherited very little ($\leq 10\%$ of normal) parental vacuole. (Solid bars) Buds that received no detectable vacuole from the mother cell. Similar results were obtained with an additional six (*act1-ΔDSE*) and four (*act1-105*) tetrads (not shown).

Table II. Relationship of Vacuole Inheritance Phenotypes to Previously Reported Defects in Actin Mutants

Allele	Amino acid substitution	Vacuole inheritance*	Previously reported phenotypes [†]
<i>act1-101</i>	D363A, E364A	–	ts (59) bud scar delocalization (24) delocalized actin patches (24) short/faint actin cables (24) minor nuclear inheritance defect (24) clumped mitochondria (24)
<i>act1-102</i>	K359A, E361A	+	wt growth (59)
<i>act1-105</i>	E311A, R312A	–	ts, cs (59)
<i>act1-111</i>	D222A, E224A, E226A	–	ts (59) bud scar delocalization (24) delocalized actin patches (24) thin actin cables (24) nuclear inheritance defect (24) morphological defects (24)
<i>act1-121</i>	E83A, K84A	+	ts, cs (59) morphological defects (24) delocalized actin patches (24) actin bars (24) minor nuclear inheritance defect (24)
<i>act1-122</i>	D80A, D81A	+	cs, ts (59)
<i>act1-133</i>	D24A, D25A	–	cs, ts (59) morphological defects (24) delocalized actin patches (24) faint actin cables (24) clumped mitochondria (24) mitochondrial motility defect (45)
<i>act1-135</i>	E4A	–	wt growth (59)
<i>act1 (end7-1)</i>	G48A	+	ts (36) endocytosis (36)

* Vacuole inheritance was examined as described in Fig. 3.

[†]References for previously reported phenotypes are indicated in parentheses.

these strains. We initially examined 20 strains from the charged-to-alanine mutant collection of Wertman and colleagues (59). Strains that grew poorly or exhibited significant morphological abnormalities were omitted from further study, since these phenotypes make interpretation of our inheritance assay difficult. The strains listed in Table II are those for which vacuole inheritance was reproducibly and unambiguously scored as either normal or defective in a quantitative assay (described in the legend to Fig. 3). Two of the mutants in Table II, *act1-101* and *act1-105*, were back crossed to appropriate wild-type strains, and, as with *act1-ΔDSE*, the vacuole inheritance defect cosegregated with the mutant actin allele (Fig. 3, *b* and *c*).

The Location of Actin Cables Relative to the Vacuole Membrane Is Consistent with Actin Playing a Primary Role in Vacuole Movement

Both forms of filamentous actin, the cortical patches and the cables, undergo defined rearrangements at specific stages of the cell cycle (2, 27). The cables, which are aligned along the mother-bud axis, become visible just before bud emergence, and then disappear as the bud reaches full size and cytokinesis occurs. Vacuole inheritance also initiates early in the cell cycle (14, 55, 57). Hence, the time of appearance, position, and orientation of actin cables are consistent with a role for these cables in vacuole movement. To further explore the location of vac-

uoles relative to actin cables, double immunofluorescence labeling studies were performed. When actin and vacuole membranes are visualized simultaneously, it is evident that many of the actin cables are associated with vacuoles (Fig. 4). Three examples of cables that align along vacuoles are indicated with arrows and careful examination reveals additional actin/vacuole contacts. Moreover, in wild-type cells used here and in other studies (53), the vacuole is present in the bud concomitant with bud emergence, and it appears that even in unbudded cells, a portion of the vacuole is juxtaposed with actin cortical patches at the site of bud emergence (arrowheads in Fig. 4). These results provide compelling evidence in support of a direct role for actin in vacuole inheritance.

Actin Filaments Used for Vacuole Inheritance Are Dynamic Structures

During zygote formation in *S. cerevisiae*, a portion of each parental vacuole is transferred to the bud. Although the parental vacuoles never fuse directly, their segregation structures join in the bud and their contents mix (55). We exploited this phenomenon to gain a better understanding of the nature of the actin filaments involved in vacuole inheritance. Zygotes formed from the homozygous mating of two *act1-ΔDSE* strains fail to transfer the vacuole to the bud (Table III). If vacuole transfer requires stable actin filaments that are pre-existing in each parental strain, then in

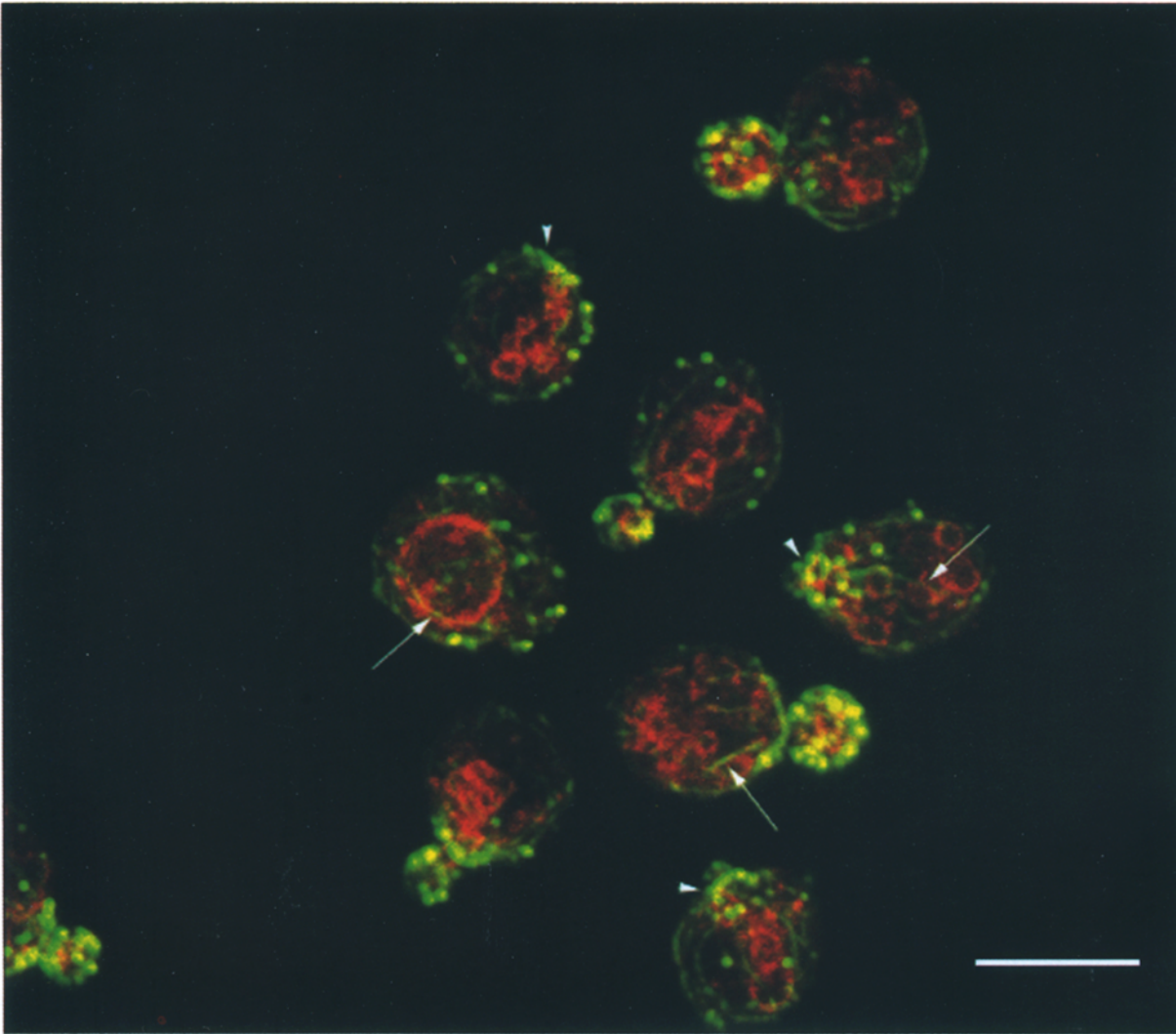


Figure 4. Actin cables directly interact with portions of the vacuole membrane. Wild-type (LWY7213) cells prepared for immunofluorescence (Materials and Methods) were simultaneously stained with anti-yeast actin (*green*) and anti-60-kD vacuolar ATPase (*red*) antibodies in order to visualize the relative subcellular locations of actin and the vacuole. Arrows indicate examples of cables lying along the vacuole membrane. Several other contacts are also visible. Arrowheads indicate future sites of bud emergence. Bar, 5 μm .

a heterozygous mating (*act1- Δ DSE* \times *ACT1*) vacuole transfer should remain defective in the *act1- Δ DSE* portion of the zygote. However, if the actin in Δ DSE filaments can exchange with wild-type actin, then wild-type actin should rescue the *act1- Δ DSE* inheritance defect. Zygotes from heterozygous matings show primarily wild-type vacuole transfer (Table III), indicating that actin from the wild-type parent can assemble into filaments in the *act1- Δ DSE* parent. This finding is correlated with *in vitro* studies which demonstrate that copolymerization of wild-type actin and Δ DSE actin increases the ability of the copolymer (relative to the Δ DSE polymer) to activate myosin S1-ATPase activity (8). Moreover, these findings suggest that actin filaments in yeast cells are in dynamic equilibrium with monomeric actin (see Discussion).

The Organelle Inheritance Defect of *act1- Δ DSE* Is Specific for the Vacuole




Cell proliferation requires proper segregation of several

types of cytoplasmic organelles. It has recently been reported that actin is required for mitochondrial (45) as well as nuclear (10, 38) inheritance in *S. cerevisiae*. The distribution of these organelles between mother cells and buds was examined in *act1- Δ DSE* and found to be qualitatively similar to wild-type (not shown). Furthermore, quantitative analysis of nuclear inheritance as a function of bud size verified that the time of nuclear migration into the bud was normal in *act1- Δ DSE* (not shown). Thus, actin's role in vacuole inheritance can be distinguished from its role in the inheritance of other organelles. These findings are consistent with earlier observations that many mitochondrial inheritance mutants exhibit normal vacuole inheritance, and likewise, that mitochondrial inheritance is normal in several vacuole partitioning mutants (34, 44, 58).

The Vacuole Inheritance Defect in *act1- Δ DSE* Is Not Due to Mislocalization of Vacuolar Proteins

We and others have reported the isolation of vacuole in-

Table III. Wild-type Actin Rescues the *act1-ΔDSE* Vacuole Inheritance Defect in Heterozygous Zygotes

			
	%	%	%
LWY1412 × LWY1425 (n = 115)	89	6	5
LWY1419 × LWY1408 (n = 111)	1	0	99
LWY1412 × LWY1419 (n = 142)	70	13	17
LWY1419 × LWY1412 (n = 96)	73	18	9

For each cross the strain written first was labeled and then mated with an unlabeled strain of the opposite mating type. The table shows the percentage of zygotes with the indicated distribution of labeled vacuoles. Each cross was performed two to three times and the total number of zygotes scored is indicated in parentheses.

heritance mutants (44, 53, 58). A subset of these mutants exhibit defects in vacuole protein sorting (58). Likewise, several mutants isolated on the basis of defects in vacuole protein sorting were subsequently found to be defective in vacuole inheritance (40, 41). The vacuole protein sorting pathway overlaps with the secretory pathway and endocytosis. Moreover, actin functions in both secretion and endocytosis in *S. cerevisiae* (29, 36, 37). Thus, it is conceivable that the *vac* phenotype associated with the *act1-ΔDSE* mutation might be an indirect result of defective vacuole protein sorting. To test this possibility, we performed pulse-chase analysis of the synthesis of two vacuolar proteins. In the *act1-ΔDSE* mutant, carboxypeptidase Y is properly targeted to the vacuole and is converted to its mature size with approximately the same kinetics as in wild-type cells (Fig. 5). A similar analysis of proteinase A synthesis confirmed that it too is targeted and processed normally (not shown). These results demonstrate that the

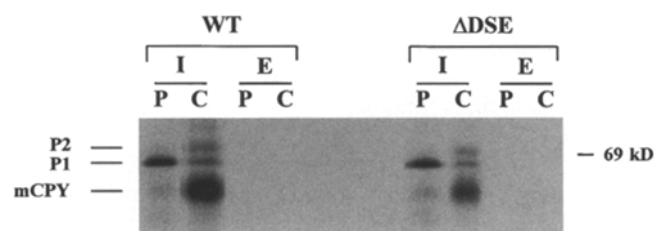


Figure 5. The vacuole inheritance defect in *act1-ΔDSE* cells is not due to mislocalization of vacuolar proteins. Spheroplasts from log-phase cultures of wild-type and *act1-ΔDSE* cells were pulse-labeled with Trans³⁵S-label for 10 min and then chased for 30 min as described in Materials and Methods. Aliquots taken before (P) and after (C) the chase period were separated into intracellular (I) and extracellular (E) fractions by centrifugation, and then precipitated with trichloroacetic acid. Carboxypeptidase Y was immunoprecipitated from each fraction and analyzed by SDS-PAGE 11% and fluorography. p1, p2, and mCPY refer to the ER-modified, Golgi-modified, and mature forms of carboxypeptidase Y, respectively. A similar analysis of Proteinase A synthesis revealed that it too is processed normally in *act1-ΔDSE* cells.




act1-ΔDSE inheritance defect is not the result of a general error in vacuole protein sorting.

A Class V Myosin Functions in Vacuole Inheritance

To further characterize the role played by actin in vacuole partitioning, we examined yeast strains carrying mutations in genes that encode known actin-binding proteins. We were particularly interested in the class V unconventional myosins, which are actin-based molecular motors implicated in organelle transport in a variety of organisms (47). Two class V myosins (Myo2p and Myo4p) have been identified in *S. cerevisiae* (17, 23). Both of these proteins function in the asymmetric localization of cellular components between the mother cell and the bud. The *Myo4* gene product is required for the daughter cell-specific localization of Ash1p, a negative regulator of HO expression (22). Myo2p activity is required for polarized growth (7, 15, 23, 32). Time course studies with a temperature-sensitive *Myo2* mutant (*myo2-66*) showed that a short shift to the restrictive temperature leads to the accumulation of small cytoplasmic vesicles, 80–100 nm in diameter, that are specifically localized to the mother cell and are not present in the bud (15, 23). Paradoxically, under these same conditions, many secreted and vacuolar proteins are properly targeted with wild-type kinetics, indicating that transport of many secretory pathway vesicles is unimpaired. It was concluded that Myo2p function is required for transporting a subset of cytoplasmic vesicles specifically from the mother cell into the bud, although the cargo in these vesicles remains unknown (15). As described below, our current studies indicate that Myo2p is also required for the transport of the vacuole into the bud.

The *myo2-66* mutation encodes an amino acid substitution in the actin-binding domain of Myo2p (32). As shown in Table IV, this mutation is associated with a defect in vacuole inheritance (even at the permissive temperature). This defect is rescued by transformation with the wild-type *MYO2* gene. No vacuole inheritance defect was observed in a *myo4Δ* deletion mutant (not shown). Most *myo2-66* cells exhibit a normal actin cytoskeleton at the permissive

Table IV. A Class V Myosin Is Required for Vacuole Inheritance

			
	%	%	%
Strain			
21R (<i>MYO2</i>) (n = 53)	87	6	7
JP7A (<i>myo2-66</i>) (n = 50)	8	6	86
LWY1656 (<i>myo2-66</i> + pMYO2) (n = 68)	74	13	13
LWY1657 (<i>myo2-66</i> + pMYO2) (n = 68)	71	12	17

Vacuole inheritance was examined as described in Fig. 3. LWY1656 and LWY1657 are independent Ura^r transformants generated by transformation of JP7A with the wild-type *MYO2* gene on a URA3, CEN plasmid (23), and were grown in SC-ura medium before labeling. Random fields of cells were examined and the percentage of cells with the indicated inheritance phenotype is shown. The total number of cells examined is given in parentheses.

temperature (23, 32) (Catlett, N.L., and L.S. Weisman, unpublished observations), yet nearly 100% display a vacuole inheritance defect. Therefore, the *myo2-66* mutation does not simply perturb vacuole transport by grossly disrupting the actin cytoskeleton.

Consistent with a role for myosin in vacuole partitioning, is the observation that three actin mutations which impair vacuole inheritance (*act1-ΔDSE*, *act1-101*, and *act1-135*) specify changes in regions of actin that are important for myosin binding (46, 48). Moreover, we observed genetic interactions between *act1-ΔDSE* and *myo2-66*. When we sought to construct a *myo2-66*, *act1-ΔDSE* double mutant, only one complete tetrad germinated out of 35 potential tetrads. Two of the spores in this tetrad contained the *myo2-66* mutation alone and two spores contained *act1-ΔDSE* alone. In most of the incomplete tetrads, we could unambiguously surmise the genotype of the missing strains, and these were predicted to have the genotype *act1-ΔDSE*, *myo2-66*. One strain, obtained from an incomplete tetrad, was *act1-ΔDSE*, *myo2-66*. However, this strain grew extremely poorly even at 24°C. We were able to successfully construct a heterozygous diploid from this strain that yielded meiotic progeny with single mutations, either *act1-ΔDSE* alone or *myo2-66* alone. However, again none of the new progeny were *act1-ΔDSE*, *myo2-66* double mutants. Hence, the *myo2-66* and *act1-ΔDSE* mutations are at least synthetically sick, if not synthetically lethal. This synthetic interaction is consistent with the hypothesis that Myo2p interacts with the amino terminus of actin (46), and supports the idea that the *vac* defect observed in *myo2-66* relates to Myo2p functioning in conjunction with actin.

In small budded cells, much of the Myo2p is localized to the tips of emerging buds (7, 32). To further explore the relationship between Myo2p and vacuole movement, we sought to determine where Myo2p resides in the cell, relative to vacuole membranes. Double label immunofluorescence studies were performed on yeast zygotes because of their large cell size relative to haploids. We observed that small budded cells and small budded zygotes contained both Myo2p caps and vacuoles that extend all the way to the cap (Fig. 6). Examples of small buds are indicated with arrowheads. Notice that in each case, coincident with the Myo2p cap, there is vacuole membrane (Fig. 6). Lillie and Brown (32) found that in addition to the Myo2p caps on the bud, low levels of Myo2p were found distributed throughout the mother cell. We note that on the vacuole membrane there are small spots of yellow that indicate regions of Myo2p, vacuole membrane colocalization. A few examples of these spots are indicated with small arrows (Fig. 6, *c* and *d*). Due to the large volume occupied by vacuole in the cytoplasm, some apparent colocalization of cytoplasmic Myo2p and vacuoles is expected. However, a close examination of Fig. 6 reveals that the most intense Myo2p staining in parental cells is almost always coincident with the vacuole membrane. (See for example the upper-left-most zygote in panel *C*, as well as the enlarged zygote in panel *D*.) The location of Myo2p relative to the vacuole membrane strongly supports the hypothesis that Myo2p is directly involved in vacuole partitioning.

In earlier papers we described populations of yeast where soon after bud emergence, the bud did not contain a vacuole (55, 57). However in the wild-type strain we are

currently using, vacuoles are present in buds concomitant with bud emergence (for example see Fig. 4 in Wang et al., 1996). Our current wild-type strains are derived from SEY6210 (42). This strain was developed by Emr and co-workers and is extensively used in his laboratory, as well as by several other investigators whose work focuses on vacuolar cell biology. To examine localization of Myo2p in the case where the vacuole has not yet extended to the tip of the small budded cell, double label immunofluorescence studies were performed with DBY1398, the wild-type strain used in our earlier studies (Fig. 7). We observe that, as found in our current wild-type strains, the Myo2p cap is located at the site of bud emergence and on tips of small buds. In cells with fully extended segregation structures, colocalization of the vacuole with Myo2p occurs in the bud tip as demonstrated in other strains (not shown, see Fig. 6). Interestingly, Myo2p also localizes to the tip of the extending segregation structure (arrowhead in Fig. 7). This localization of Myo2p on both the tip of the segregation structure and the bud tip is consistent with a role for Myo2p in both the directed transport of vacuoles and other vesicles into the bud. Note that there is some vacuolar membrane in the bud, but it is likely that this would not have been detected with the fluorescein derivatives (39, 57) used in previous studies.

Actin-Profilin Interactions Are Important for Vacuole Inheritance

Profilin is an actin-binding protein that is an important regulator of actin filament assembly. Two of the actin alleles associated with vacuole inheritance defects (*act1-101* and *act1-111*) have been shown to inhibit the interaction of actin with profilin *in vivo*, via the “two-hybrid” assay (4). Furthermore, Glu364 (which is changed to Ala in *act1-101*) contacts profilin in the actin-profilin cocrystal structure (43) and has been cross-linked to profilin *in vitro* (49). The overlap between amino acids in actin that are important for both vacuole partitioning and profilin binding, suggests that actin-profilin interactions may be important for the function of actin in vacuole inheritance. We examined a yeast strain (BHY31) carrying a mutation in the profilin gene. The *pfy1-112* mutation specifies an amino acid substitution (R76G) (18) in a region of profilin that contributes to one of the primary contacts between profilin and actin (43). This mutation gives rise to a *vac* phenotype (Fig. 8) without disrupting actin localization or producing any other discernible phenotypes (18). It is not immediately clear what role profilin might play in vacuole partitioning. However, given the dynamic nature of actin filaments used for vacuole transfer (see above), the role of profilin in regulating filament assembly may be critical to the function of these filaments in vacuole inheritance.

The crystal structure of the bovine profilin-actin complex demonstrates two major contact sites (43). One contact includes a salt bridge between R74 of bovine profilin (analogous to R72 or R76 of yeast profilin based on sequence alignment) and the COOH-terminal carboxylate group of actin. The other contact includes a salt bridge between K112 of profilin and E364 of actin. Interestingly, the *pfy1-112* mutation (R76A) alters a profilin amino acid that participates in the first salt bridge, while the *act1-101* mu-

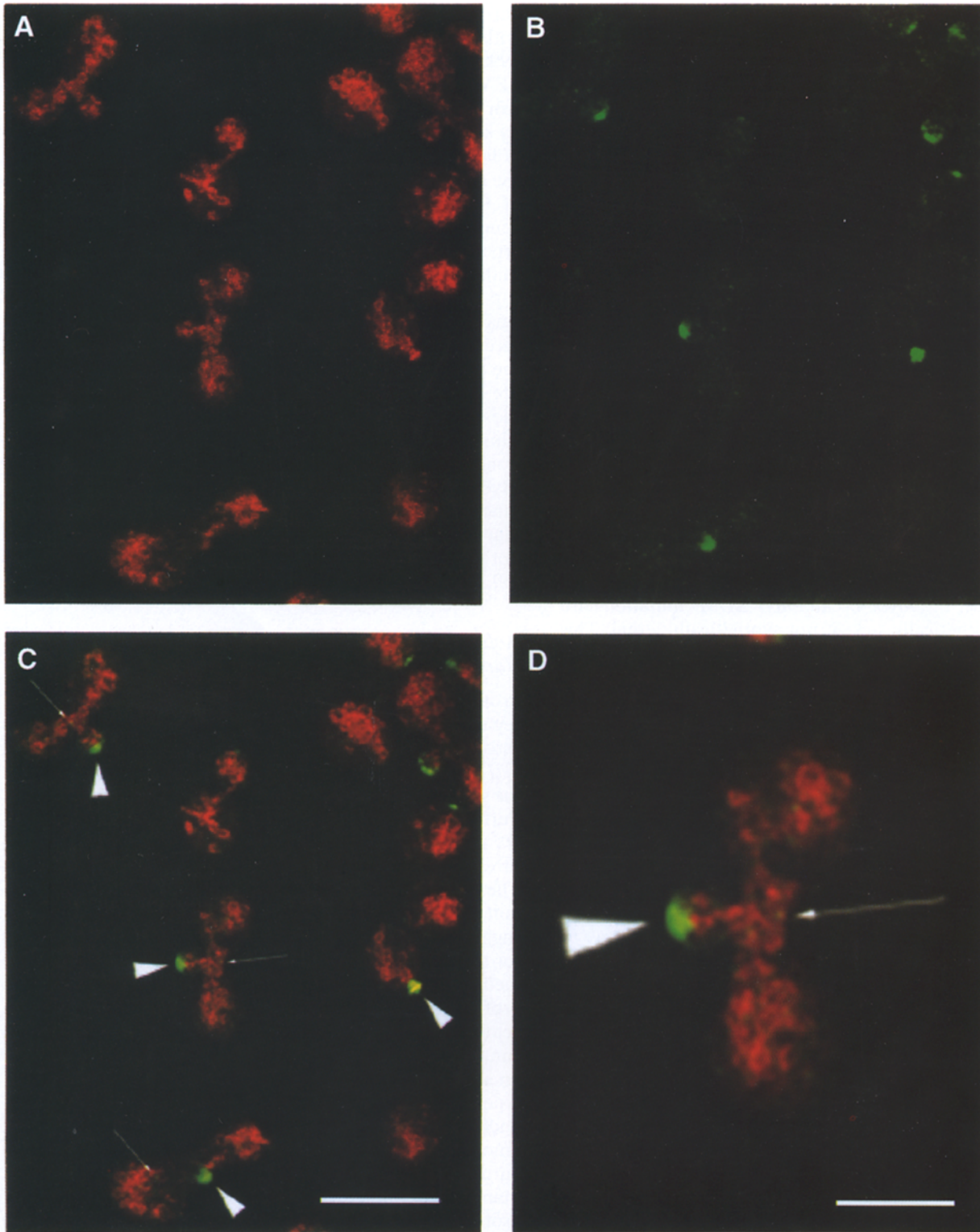


Figure 6. Specific regions of the vacuole colocalize with Myo2p. Wild-type zygotes (from mating of X2180-1A and X2180-1B, Yeast Genetic Stocks Center) were prepared for immunofluorescence and stained with anti-Myo2p (*green*) and anti-60-kD vacuolar ATPase (*red*) antibodies in order to simultaneously visualize Myo2p and the vacuolar membrane (see Materials and Methods). (A) 60 kD ATPase, (B) Myo2p, (C) combined image; regions where the vacuole membrane and Myo2p overlap appear yellow-green or yellow. The arrowheads in C and D indicate four examples of small buds with the Myo2p cap clearly colocalizing with a portion of the vacuole membrane. Arrows in C and D point to examples of small Myo2p spots along the vacuole membrane. (D) Enlarged view of zygote from (C). Bars: (C) 10 μ m. (D) 2.5 μ m.

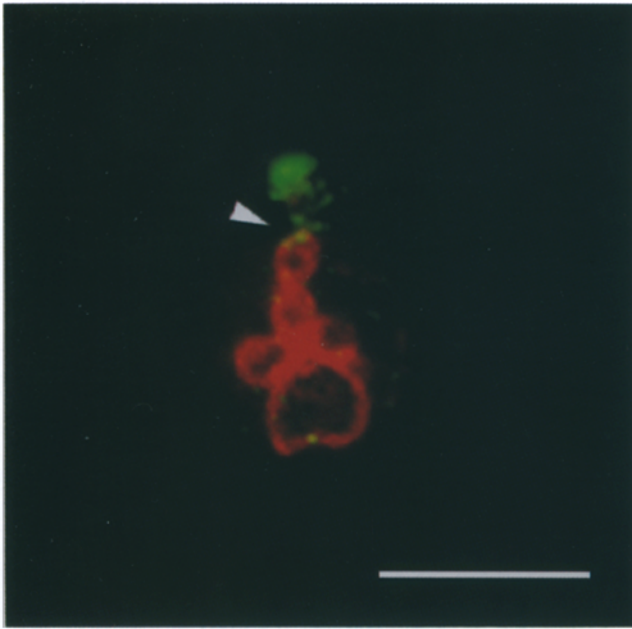


Figure 7. Myo2p is localized at the tip of the extending segregation structure. DBY1398 cells grown to mid-log phase were prepared for immunofluorescence and stained with anti-Myo2p (green) and anti-60-kD vacuolar ATPase (red) in order to simultaneously visualize Myo2p and the vacuolar membrane. An arrowhead indicates the segregation structure. Bar, 5 μ m.

tation (D363A, E364A) changes an actin amino acid involved in the second contact site. To further investigate the role of actin-profilin interactions in vacuole inheritance, we sought to construct a profilin-actin double mutant. A strain carrying the *pfy1-112* mutation marked with *LEU2* (situated next to the 3' end of the profilin gene) was crossed to a strain carrying the *act1-101* mutation marked with *HIS3* (situated next to the 3' end of the actin gene). Of 24 tetrads dissected, only one viable *Leu*⁺/*His*⁺ spore was identified, indicating a synthetic lethality between the *pfy1-112* and *act1-101* mutations. (The one viable *Leu*⁺, *His*⁺ spore probably arose through a recombination event between the *pfy1* or *act1* structural gene, and the corresponding marker gene.) Thus, disruption of either contact-site alone impairs vacuole inheritance, without other discernible defects. However, disruption of both is lethal.

Discussion

Transfer of the Yeast Vacuole into the Bud during Cell Division Is Mediated by the Actin Cytoskeleton

In the present work we provide the first demonstration that a specific cytoskeletal component, actin, is required for vacuole transport in dividing yeast cells. Since a variety of functions have previously been ascribed to the actin cytoskeleton of *S. cerevisiae* (10, 29, 37), it is important to differentiate between a direct or indirect role for actin in vacuole inheritance. Several lines of evidence support a direct role. (a) Most of the actin mutants that have vacuole inheritance defects exhibit normal morphology and bud growth. (b) In the *act1- Δ DSE* mutant the vacuole inheri-

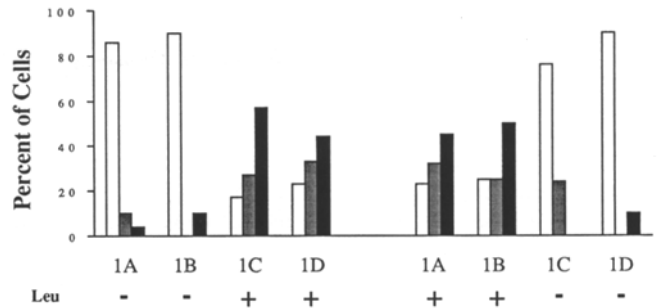


Figure 8. An amino acid substitution (R76G) in a region of profilin that forms a contact with actin disrupts vacuole inheritance. A strain carrying the *pfy1-112* profilin allele linked to the *LEU2* gene (BHY31) was back-crossed to a wild-type strain with the same genetic background (DC5). The resulting diploid was sporulated and examined for the presence of the wild-type (*Leu*⁻) or *pfy1-112* (*Leu*⁺) profilin allele. Vacuole inheritance was examined as described in Fig. 3. (Open bars) Buds that inherited normal amounts of the parental vacuole. (Stippled bars) Buds that inherited very little ($\leq 10\%$ of normal) parental vacuole. (Solid bars) Buds that received no detectable vacuole from the mother cell. Similar results were obtained with four additional tetrads (not shown).

tance defect occurs in the absence of any defects in vacuole protein sorting or F-actin localization. (c) Wild-type actin rapidly suppresses the *act1- Δ DSE* inheritance defect in heterozygous zygotes. (d) This suppression correlates with the ability of wild-type actin to attenuate defects of Δ DSE actin in vitro (8). (e) The time and position of vacuole transfer coincide with the formation of actin cables during the cell cycle (27). (f) Indeed, double label immunofluorescence studies show a close association of vacuole membranes and actin cables. (g) The rate of vacuole movement, 0.1–0.2 μ m/s (Weisman, L.S., unpublished observation), is consistent with rates of other actin-based motility events (6, 30). We therefore suggest that actin functions directly in vacuole inheritance, presumably serving as a track that allows for the precise delivery of the vacuole first to the site of bud emergence, and then from the mother cell into the bud.

Vacuole Inheritance Is Defective in a Variety of Actin Mutants

Several *act1* mutants exhibit a vacuole inheritance defect (Table II). When considered in the context of available structural data, these results offer insight into the mechanism by which actin facilitates vacuole inheritance. For example, *act1- Δ DSE*, *act1-101*, and *act1-135* each alter residues that are important for actin-myosin interactions (46, 48). The E364A substitution in *act1-101* is also predicted to destroy one of two primary contact sites between actin and profilin (43), and has recently been shown to impair actin-profilin interactions in a two-hybrid assay (4). The *vac* phenotypes of these mutants might therefore arise from the requirement for myosin and profilin function in vacuole inheritance. The *act1-102* and *act1-111* mutations also block the binding of profilin to actin in a two hybrid assay (4). While *act1-111* displays a *vac* phenotype, *act1-102* does not. This presumably reflects a difference in the

requirements for interaction in the two-hybrid assay vs function in vacuole inheritance. In this regard, it is worth noting that the *act1-102* mutation also does not exhibit the temperature-sensitive growth phenotype that is associated with other mutations at profilin contact sites (59).

The *act1-105* mutation has previously been shown to block interactions between actin and Srv2p, a bifunctional protein that functions in Ras-mediated signal transduction and actin cytoskeleton organization (4, 11, 12, 52). The *vac* phenotype of this mutant may represent further demonstration of the functional overlap between Srv2p and profilin (52). Finally, although the amino acids altered by the *act1-133* mutation have not specifically been implicated in binding to any particular protein, this mutation disrupts actin cables and is associated with defects in mitochondrial localization and motility (10, 45). Hence, the *vac* phenotype associated with *act1-133* may result from a more general defect in the actin cytoskeleton.

Actin functions in a wide variety of cellular processes. These activities generally require interactions with specific proteins that use overlapping and/or distinct binding sites on the actin molecule (4). Therefore, it is not surprising that vacuole inheritance is normal in some mutants with defects in other membrane trafficking pathways (e.g., *end7-1*) or that exhibit temperature sensitive growth (e.g., *act1-121* and *act1-122*). Likewise, it is to be expected that some actin mutations that block vacuole inheritance do not lead to other discernible phenotypes (e.g., *act1-135* in Table II).

Actin Cables Colocalize with Vacuole Membranes

Simultaneous indirect immunofluorescence localization of both filamentous actin and vacuole membranes reveals that many actin cables within the mother cell are associated with vacuole membranes. This association is most prominent immediately before and during vacuole partitioning. Notably, in unbudded cells with actin cortical patches organized at the site of bud emergence, a portion of the mother vacuole is also localized to that area. It appears that this region of the vacuole then transits into the bud as the bud emerges. These observations of the location of the vacuole just before bud emergence, are quite similar to what has been observed for other endomembranes (for review see reference 9). Colocalization of actin with the vacuole membrane corroborates the genetic evidence suggesting that actin is directly involved in vacuole inheritance.

Myo2p Is Involved in Vacuole Inheritance

Myo2p is a class V unconventional myosin that is required for polarized growth in *S. cerevisiae* (23). This requirement has been attributed to its proposed role in the transport of small cytoplasmic vesicles from the mother cell into the bud (15, 23). Several observations suggest that Myo2p also functions in vacuole inheritance. (a) A temperature-sensitive mutation in the actin-binding domain of Myo2p blocks vacuole inheritance, even at the permissive temperature. This defect is observed in essentially all cells and is not due to a disruption of the actin cytoskeleton. (b) The *myo2-66* mutation does not affect other actin-dependent membrane trafficking pathways known to intersect with the vacuole

(15). (c) Several actin mutations that impair vacuole inheritance occur in regions of actin that are important for myosin binding. (d) The effect of the *act1-ΔDSE* mutation on vacuole transport in vivo is correlated with a decrease in the ability of ΔDSE-actin to activate myosin ATPase activity in vitro (8). (e) There are genetic interactions between *act1-ΔDSE* and *myo2-66*. (f). Myo2p colocalizes with vacuole membranes.

By analogy with the generalized role of class V myosins in vesicle transport in other systems (47), we propose that yeast Myo2p acts as a molecular motor to facilitate movement of the vacuole along actin filaments into newly emerging buds (Fig. 9). The location of both actin and Myo2p relative to the vacuole are consistent with this model. We suggest that Myo2p functions relatively early in vacuole partitioning, working both before bud emergence

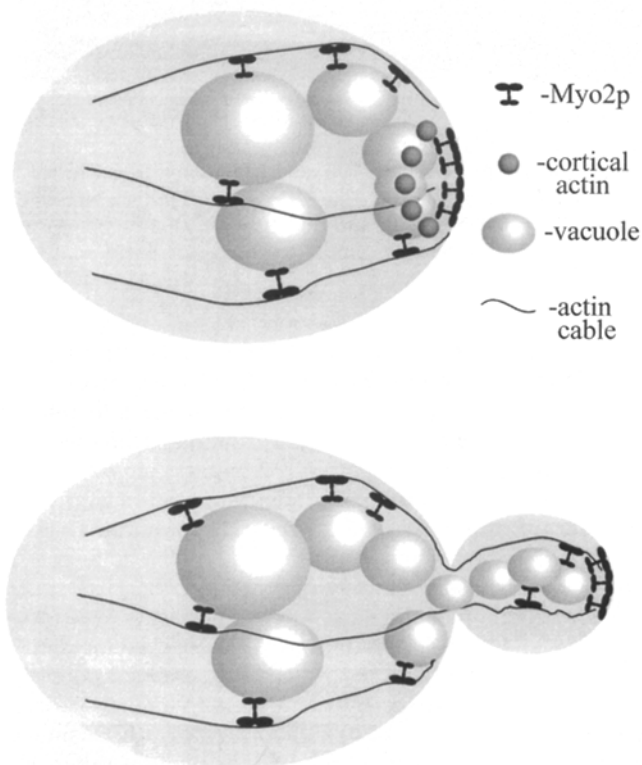


Figure 9. Suggested model for actin-mediated vacuole inheritance in *S. cerevisiae*. In an unbudded cell (top) the vacuole (gray) is an oval, lobed structure and is associated with actin cables (black lines) (see Fig. 4). Myo2p (black, multi-lobed structure) may be acting as a motor, attached to both the vacuole and actin cables. (Some of the Myo2p is distributed in the mother cell and is often found colocalized with vacuole membrane [Figs. 6 and 7]). Most of the Myo2p is found in a cap at the site of bud emergence (7, 32) (Figs. 6 and 7). Cortical actin patches (small dark balls) are found at the plasma membrane and are present at the site of bud emergence (10). As the bud emerges, actin cables extend into the bud, as does the vacuole. Also at this time, the vacuolar segregation structure forms and may be transported by myosin along the actin filaments. As the bud enlarges, vacuole transfer continues until nuclear migration begins (not shown). For simplicity, other organelles are not depicted, also actin cortical patches in the small bud are not shown. For a discussion of other roles for Myo2p, see Results and Discussion.

and also in small budded cells. This is based on the observation that vacuoles are juxtapositioned with both actin cortical patches (Fig. 4) and Myo2p caps (Fig. 6) at the site of bud emergence in as yet unbudded cells. One question that arises is why does Myo2p accumulate at caps in the bud? It may be that this location corresponds to other functions of Myo2p, which is also required for polarized growth (15, 23). Alternatively, perhaps these caps do not reflect the site of Myo2p function, but rather are the site that Myo2p resides after it has brought its cargo both to the site of bud emergence and also into the emerging bud. Unlike microtubule-dependent motility, all actin-dependent myosin-mediated vesicle movements characterized to date occur exclusively toward the barbed end of actin filaments (31). In this scenario, Myo2p would be moving along actin cables that have a single polarity and thus allow movement in a single direction. Once Myo2p arrives at the bud tip, it would not be able to go in the reverse direction. An alternative model to explain the location of Myo2p caps is that the protein is not working as a conventional motor, but rather is forming a site for the attachment and organization of actin cables and vacuoles. Our finding that Myo2p is found on the mother cell vacuole membrane is more consistent with the first model.

We also cannot rule out the possibility that Myo2p functions to target another protein to a specific subcellular location, and that proper targeting of this protein is required for partitioning of the vacuole and for polarized growth. Such a model would be consistent with the observation that *myo2-66* is synthetically lethal with several late-acting *sec* mutations (15, 33). However, we favor the idea of a direct role for the reasons discussed above, and because the targeting of several proteins to a variety of subcellular locations have all been shown to be normal in *myo2-66*, even at the restrictive temperature (15, 23).

In a detailed analysis of the *myo2-66* mutant by electron microscopy, Govindan and coworkers observed small (80–100 nm diameter) vesicles that accumulate in mother cells (but not in buds) after a short shift to the restrictive temperature (15). No secretory defect was observed and the identity of the vesicles could not be determined. Because early (but not late) *SEC* genes are required for their formation, the authors speculated that the 80–100-nm vesicles represent a subset of late secretory vesicles, or that they result from a defect in the inheritance of the Golgi complex. Based on those observations and our results presented here, we suggest that the latter possibility be explored further. Perhaps the *myo2-66* vesicles correspond to a heritable unit of the organelles in the secretory pathway (e.g., the Golgi) and Myo2p function is required for targeting them specifically to the bud. The fact that transport of the 80–100-nm vesicles is blocked only at the restrictive temperature, while vacuole inheritance is defective at the permissive temperature may reflect their relative sizes, since transport of the vacuole is expected to be more physically demanding than transport of much smaller vesicles.

Actin Filaments That Function in Vacuole Transport Are Dynamic Structures

Examination of vacuole inheritance in newly formed zygotes allowed us to probe the capacity of the yeast actin

cytoskeleton to undergo dynamic rearrangements during the cell cycle. In wild-type yeast zygotes, portions of each parental vacuole are transferred to the bud as well as to the other parent (55). This vacuole transfer event occurs normally in *act1-ΔDSE/ACT1* zygotes, but not in *act1-ΔDSE/act1-ΔDSE* zygotes (Table III). Normal vacuole transfer in the heterozygote indicates that actin from the wild-type parent is able to assemble into filaments in the *act1-ΔDSE* parent. This actin is probably derived from a pre-existing source in the wild-type parent rather than from de novo expression of the wild-type gene, since the defect is rescued shortly after zygote formation and it is unlikely that gene expression in the newly formed diploid nucleus has contributed enough actin to rescue the defect. This argument is supported by the fact that many other recessive *vac* mutants are not rescued in this assay (53, 58).

Recently, Karpova and coworkers examined the relative abundance of filamentous and monomeric actin in yeast cells (26). They discovered that the majority of actin in wild-type cells exists as polymerized filaments, and that the steady-state level of free actin monomers is very low. Our zygote studies therefore imply that yeast actin filaments can be disassembled into soluble monomers that are able to diffuse into both parents of the zygote and be incorporated into filaments required for vacuole transfer. The coordination of vacuole transfer with the cell cycle implies that actin filament rearrangement is a regulated process and therefore protein-mediated. If this is indeed the case, it might explain the involvement of profilin in vacuole inheritance (Fig. 8), since profilin is thought to regulate actin filament assembly.

Summary

We have demonstrated the involvement of actin and myosin in vacuole inheritance. In addition to providing insights into the molecular mechanisms of this process, our results present a new *in vivo* assay for monitoring actin and myosin function. Unlike other functions ascribed to yeast actin (e.g., endocytosis and secretion), vacuole partitioning can be easily visualized in living cells. Moreover, the distance that the vacuole moves in yeast zygotes, over 5 μm , suggests that even subtle differences in rates of movement may be detected.

We thank Dan L. Morris for preliminary studies on the rate of vacuole movement in yeast zygotes. We are very grateful to Dr. Peter Rubenstein for providing us with the *act1-ΔDSE* mutant and for the numerous discussions that led to this project. We thank Drs. Sue Lillie and Susan Brown for generously providing us with anti-actin antiserum, affinity-purified Myo2p antibody, and for many helpful discussions. We thank Dr. Xin Chen for purification of the anti-actin antibody. We thank Drs. Kenneth Wertman, David Drubin, and David Botstein for generously sending us their set of charged-to-alanine actin alleles. We thank Dr. Brian Haarer for providing strains with profilin point mutations in advance of their publication, Drs. Bruce Horazdovsky and Scott Emr for the polyclonal antisera against carboxypeptidase Y and proteinase A, and Dr. Gerald Johnston for the *myo2-66* mutant and *MYO2* plasmid. We thank Paul Millard and Molecular Probes for samples of Oregon Green conjugates. We thank Justin Fishbaugh and the University of Iowa Flow Cytometry Facility for the fluorescence-activated cell sorting analyses, and Tom Monninger and the University of Iowa Central Microscopy Research Facility for guidance in use of the confocal microscope. Finally, we thank Michelle Muller and Emily Bristow for excellent technical assistance and

Drs. Robert Cohen and Rachelle Crosbie for helpful discussions. L.S. Weisman is a Carver Research Scientist.

This work was supported by a gift to L.S. Weisman from the Roy J. Carver Charitable Trust, National Institutes of Health (NIH) grant GM50403 to L.S. Weisman, and an NIH Training grant DK07690 to K.L. Hill.

Received for publication 26 March 1996 and in revised form 18 September 1996.

References

1. Adams, A.E.M., and J.R. Pringle. 1984. Relationship of actin and tubulin distribution to bud growth in wild-type and morphogenetic-mutant *Saccharomyces cerevisiae*. *J. Cell Biol.* 98:934–945.
2. Adams, A.E., and J.R. Pringle. 1991. Staining of actin with fluorochrome-conjugated phalloidin. *Methods Enzymol.* 194:729–731.
3. Allen, R.D., D.G. Weiss, J.H. Hayden, D.T. Brown, H. Fujiwake, and M. Simpson. 1985. Gliding movement of and bidirectional transport along single native microtubules from squid axoplasm: evidence for an active role of microtubules in cytoplasmic transport. *J. Cell Biol.* 100:1736–1752.
4. Amberg, D.C., E. Basart, and D. Botstein. 1995. Defining protein interactions with yeast actin in vivo. *Nat. Struct. Biol.* 2:28–35.
5. Ault, J.G., and C.L. Rieder. 1994. Centrosome and kinetochore movement during mitosis. *Curr. Opin. Cell Biol.* 6:41–49.
6. Bearer, E.L., J.A. DeGiorgis, R.A. Bodner, A.W. Kao, and T.S. Reese. 1993. Evidence for myosin motors on organelles in squid axoplasm. *Proc. Natl. Acad. Sci. USA.* 90:11252–11256.
7. Brockerhoff, S.E., R.C. Stevens, and T.N. Davis. 1994. The unconventional myosin, Myo2p, is a calmodulin target at sites of cell growth in *Saccharomyces cerevisiae*. *J. Cell Biol.* 124:315–323.
8. Cook, R.K., W.T. Blake, and P.A. Rubenstein. 1992. Removal of the amino-terminal acidic residues of yeast actin. Studies in vitro and in vivo. *J. Biol. Chem.* 267:9430–9436.
9. Drubin, D.G., and W.J. Nelson. 1996. Origins of cell polarity. *Cell.* 84:335–344.
10. Drubin, D.G., H.D. Jones, and K.F. Wertman. 1993. Actin structure and function: roles in mitochondrial organization and morphogenesis in budding yeast and identification of the phalloidin-binding site. *Mol. Biol. Cell.* 4:1277–1294.
11. Fedor-Chaikin, M., R.J. Deschenes, and J.R. Broach. 1990. SRV2, a gene required for RAS activation of adenylate cyclase in yeast. *Cell.* 61:329–340.
12. Gerst, J.E., K. Ferguson, A. Fojtek, M. Wigler, and J. Field. 1991. CAP is a bifunctional component of the *Saccharomyces cerevisiae* adenylate cyclase complex. *Mol. Cell Biol.* 11:1248–1257.
13. Gietz, R.D., A. Jean, R.A. Woods, and R.H. Schiestl. 1992. Improved method for high efficiency transformation of intact yeast cells. *Nucleic Acids Res.* 8:1425.
14. Gomes de Mesquita, D.S., R. ten Hoopen, and C.L. Woldringh. 1991. Vacuolar segregation to the bud of *Saccharomyces cerevisiae*: an analysis of morphology and timing in the cell cycle. *J. Gen. Microbiol.* 137:2447–2454.
15. Govindan, B., R. Bowser, and P. Novick. 1995. The role of Myo2, a yeast class V myosin, in vesicular transport. *J. Cell Biol.* 128:1055–1068.
16. Guthrie, B.A., and W. Wickner. 1988. Yeast vacuoles fragment when microtubules are disrupted. *J. Cell Biol.* 107:115–120.
17. Haarer, B.K., A. Petzold, S.H. Lillie, and S.S. Brown. 1994. Identification of MYO4, a second class V myosin gene in yeast. *J. Cell Sci.* 107:1055–1064.
18. Haarer, B.K., A.S. Petzold, and S.S. Brown. 1993. Mutational analysis of yeast profilin. *Mol. Cell Biol.* 13:7864–7873.
19. Haas, A., and W. Wickner. 1996. Homotypic vacuole fusion requires Sec17p (yeast Alpha-SNAP) and Sec18p (yeast NSF). *EMBO (Eur. Mol. Biol. Organ.) J.* 15:3296–3305.
20. Haas, A., D. Scheglmann, T. Lazar, D. Gallwitz, and W. Wickner. 1995. The GTPase of *Saccharomyces cerevisiae* is required on both partner vacuoles for late-stage homotypic membrane-fusion during vacuole inheritance. *EMBO (Eur. Mol. Biol. Organ.) J.* 14:5258–5270.
21. Horazdovsky, B.F., and S.D. Emr. 1993. The vps16 gene product associates with a sedimentable protein complex and is essential for vacuolar protein sorting in yeast. *J. Biol. Chem.* 268:4953–4962.
22. Jansen, R.-P., C. Dowzer, C. Michaelis, M. Galova, and K. Nasmyth. 1996. Mother cell-specific HO expression in budding yeast depends on the unconventional myosin Myo4p and other cytoplasmic proteins. *Cell.* 84:687–697.
23. Johnston, G.C., J.A. Prendergast, and R.A. Singer. 1991. The *Saccharomyces cerevisiae* MYO2 gene encodes an essential myosin for vectorial transport of vesicles. *J. Cell Biol.* 113:539–551.
24. Jones, H.D., M. Schliwa, and D.G. Drubin. 1993. Video microscopy of organelle inheritance and motility in budding yeast. *Cell Motil. Cytoskeleton.* 25:129–142.
25. Kaiser, C., S. Michaelis, and A. Mitchell. 1994. Methods in Yeast Genetics. Cold Spring Harbor Laboratory Press.
26. Karpova, T.S., K. Tatchell, and J.A. Cooper. 1995. Actin filaments in yeast are unstable in the absence of capping protein or fimbrin. *J. Cell Biol.* 131:1483–1493.
27. Kilmartin, J.V., and A.E. Adams. 1984. Structural rearrangements of tubulin and actin during the cell cycle of the yeast *Saccharomyces*. *J. Cell Biol.* 98:922–933.
28. Klionsky, D.J., L.M. Banta, and S.D. Emr. 1988. Intracellular sorting and processing of a yeast vacuolar hydrolase: proteinase A propeptide contains vacuolar targeting information. *Mol. Cell Biol.* 8:2105–2116.
29. Kubler, E., and H. Riezman. 1993. Actin and fimbrin are required for the internalization step of endocytosis in yeast. *EMBO (Eur. Mol. Biol. Organ.) J.* 12:2855–2862.
30. Kuznetsov, S.A., G.M. Langford, and D.G. Weiss. 1992. Actin-dependent organelle movement in squid axoplasm. *Nature (Lond.)* 356:722–725.
31. Langford, G.M. 1995. Actin- and microtubule-dependent organelle motors: interrelationships between the two motility systems. *Curr. Opin. Cell Biol.* 7:82–88.
32. Lillie, S.H., and S.S. Brown. 1994. Immunofluorescence localization of the unconventional myosin, Myo2p, and the putative kinesin-related protein, Smy1p, to the same regions of polarized growth in *Saccharomyces cerevisiae*. *J. Cell Biol.* 125:825–842.
33. Liu, H., and A. Bretscher. 1992. Characterization of TPM1 disrupted yeast cells indicates an involvement of tropomyosin in directed vesicular transport. *J. Cell Biol.* 118:285–299.
34. McConnell, S.J., L.C. Stewart, A. Talin, and M.P. Yaffe. 1990. Temperature-sensitive yeast mutants defective in mitochondrial inheritance. *J. Cell Biol.* 111:967–976.
35. Mulholland, J., D. Preuss, A. Moon, A. Wong, D. Drubin, and D. Botstein. 1994. Ultrastructure of the yeast actin cytoskeleton and its association with the plasma membrane. *J. Cell Biol.* 125:381–391.
36. Munn, A.L., B.J. Stevenson, M.I. Geli, and H. Riezman. 1995. *end5*, *end6*, and *end7*: mutations that cause actin delocalization and block the internalization step of endocytosis in *Saccharomyces cerevisiae*. *Mol. Biol. Cell.* 6:1721–1742.
37. Novick, P., and D. Botstein. 1985. Phenotypic analysis of temperature sensitive yeast actin mutants. *Cell.* 40:405–416.
38. Palmer, R.E., D.S. Sullivan, T. Huffaker, and D. Koshland. 1992. Role of astral microtubules and actin in spindle orientation and migration in the budding yeast, *Saccharomyces cerevisiae*. *J. Cell Biol.* 119:583–593.
39. Pringle, J.R., R.A. Preston, A.E. Adams, T. Stearns, D.G. Drubin, B.K. Haarer, and E.W. Jones. 1989. Fluorescence microscopy methods for yeast. *Methods Cell Biol.* 31:357–435.
40. Raymond, C.K., I. Howald-Stevenson, C.A. Vater, and T.H. Stevens. 1992. Morphological classification of the yeast vacuolar protein sorting mutants: evidence for a prevacuolar compartment in class E vps mutants. *Mol. Biol. Cell.* 3:1389–1402.
41. Raymond, C.K., P.J. O'Hara, G. Eichinger, J.H. Rothman, and T.H. Stevens. 1990. Molecular analysis of the yeast *VPS3* gene and the role of its product in vacuolar protein sorting and vacuolar segregation during the cell cycle. *J. Cell Biol.* 111:877–892.
42. Robinson, J.S., D.J. Klionsky, L.M. Banta, and S.D. Emr. 1988. Protein sorting in *Saccharomyces cerevisiae*: isolation of mutants defective in the delivery and processing of multiple vacuolar hydrolases. *Mol. Cell Biol.* 8:4936–4948.
43. Schutt, C.E., J.C. Myslik, M.D. Rozycki, N.C. Goonesekere, and U. Lindberg. 1993. The structure of crystalline profilin- β -actin. *Nature (Lond.)* 365:810–816.
44. Shaw, J.M., and W.T. Wickner. 1991. *vac2*: a yeast mutant which distinguishes vacuole segregation from Golgi-to-vacuole protein targeting. *EMBO (Eur. Mol. Biol. Organ.) J.* 10:1741–1748.
45. Simon, V.R., T.C. Swayne, and L.A. Pon. 1995. Actin-dependent mitochondrial motility in mitotic yeast and cell-free systems: identification of a motor activity on the mitochondrial surface. *J. Cell Biol.* 130:345–354.
46. Sutoh, K. 1982. Identification of myosin-binding sites on the actin sequence. *Biochemistry.* 21:3654–3661.
47. Titus, M.A. 1993. From fat yeast and nervous mice to brain myosin-V. *Cell.* 75:9–11.
48. Trayer, I.P., H.R. Trayer, and B.A. Levine. 1987. Evidence that the N-terminal region of A1-light chain of myosin interacts directly with the C-terminal region of actin. A proton magnetic resonance study. *Eur. J. Biochem.* 164:259–266.
49. Vandekerckhove, J.S., D.A. Kaiser, and T.D. Pollard. 1989. Acanthamoeba actin and profilin can be cross-linked between glutamic acid 364 of actin and lysine 115 of profilin. *J. Cell Biol.* 109:619–626.
50. Vida, T.A., and S.D. Emr. 1995. A new vital stain for visualizing vacuolar membrane dynamics and endocytosis in yeast. *J. Cell Biol.* 128:779–792.
51. Vida, T.A., T.R. Graham, and S.D. Emr. 1990. In vitro reconstitution of intercompartmental protein transport to the yeast vacuole. *J. Cell Biol.* 111:2871–2884.
52. Vojtek, A., B. Haarer, J. Field, J. Gerst, T.D. Pollard, S. Brown, and M. Wigler. 1991. Evidence for a functional link between profilin and CAP in the yeast *S. cerevisiae*. *Cell.* 66:497–505.
53. Wang, Y.-X., H. Zhao, T. Harding, D. Gomes de Mesquita, C.L. Woldringh, D. Klionsky, A.L. Munn, and L.S. Weisman. 1996. Multiple classes of yeast mutants are defective in vacuole partitioning yet target vacuole proteins correctly. *Mol. Biol. Cell.* 7:1375–1389.

54. Warren, G., and W. Wickner. 1996. Organelle inheritance. *Cell*. 84:395–400.
55. Weisman, L.S., and W. Wickner. 1988. Intervacuole exchange in the yeast zygote: a new pathway in organelle communication. *Science (Wash. DC)*. 241:589–591.
56. Weisman, L.S., and W. Wickner. 1992. Molecular characterization of *VAC1*, a gene required for vacuole inheritance and vacuole protein sorting. *J. Biol. Chem.* 267:618–623.
57. Weisman, L.S., R. Bacallao, and W. Wickner. 1987. Multiple methods of visualizing the yeast vacuole permit evaluation of its morphology and inheritance during the cell cycle. *J. Cell Biol.* 105:1539–1547.
58. Weisman, L.S., S.D. Emr, and W.T. Wickner. 1990. Mutants of *Saccharomyces cerevisiae* that block intervacuole vesicular traffic and vacuole division and segregation. *Proc. Natl. Acad. Sci. USA*. 87:1076–1080.
59. Wertman, K.F., D.G. Drubin, and D. Botstein. 1992. Systematic mutational analysis of the yeast *ACT1* gene. *Genetics*. 132:337–350.
60. Xu, Z., and W. Wickner. 1996. Thioredoxin is required for vacuole inheritance in *Saccharomyces cerevisiae*. *J. Cell Biol.* 132:787–794.
61. Yaffe, M.P. 1991. Organelle inheritance in the yeast cell cycle. *Trends Cell Biol.* 1:160–164.